LAWRENCE
LIVERMORE
NATIONAL
LABORATORY

UCRL-JRNL-229669

Rampant changes in 5f 5/2 and 5f 7/2 filling across the light and middle actinide metals

K. Moore, G. van der Lann, M. Wall, A. Schwartz, R. Haire

April 4, 2007

Physical Review B

This document was prepared as an account of work sponsored by an agency of the United States Government. Neither the United States Government nor the University of California nor any of their employees, makes any warranty, express or implied, or assumes any legal liability or responsibility for the accuracy, completeness, or usefulness of any information, apparatus, product, or process disclosed, or represents that its use would not infringe privately owned rights. Reference herein to any specific commercial product, process, or service by trade name, trademark, manufacturer, or otherwise, does not necessarily constitute or imply its endorsement, recommendation, or favoring by the United States Government or the University of California. The views and opinions of authors expressed herein do not necessarily state or reflect those of the United States Government or the University of California, and shall not be used for advertising or product endorsement purposes.

Rampant changes in $5f_{5/2}$ and $5f_{7/2}$ filling across the light and middle actinide metals

K.T. Moore[1]*, G. van der Laan[2], M.A. Wall[1], A.J. Schwartz[1], R.G. Haire[3]

[1]*Lawrence Livermore National Laboratory, Livermore, California 94550, USA.*

[2]*Magnetic Spectroscopy Group, Daresbury Laboratory, Warrington WA4 4AD, UK.*

[3]*Oak Ridge National Laboratory, MS-6375, Oak Ridge, Tennessee 37831, USA.*

We examine the branching ratio of the $N_{4,5}$ ($4d \rightarrow 5f$) spectra of Th, U, Np, Pu, Am, and Cm metal using electron energy-loss spectroscopy (EELS) in a transmission electron microscope (TEM), together with many-electron atomic spectral calculations and the spin-orbit sum rule. Our results show that: 1) The actinide metals Pu, Am, and Cm exhibit intermediate coupling. 2) The intermediate coupling values for the $5f$ states as calculated using a many-electron atomic model are correct for the actinides, this being proven by our new results for curium. 3) The EELS branching ratio is sensitive to the degree of $5f$ electron delocalization, which is illustrated by the transition from *LS* to intermediate coupling between U and Pu.

PACS: 79.20.Uv, 71.10.–w, 71.27.+a, 71.70.–d

*Contact Author
Tel: 925-422-9741
Fax: 925-422-6892
Email: moore78@llnl.gov

Actinide materials are rapidly growing in importance for energy and industry, particularly given the exploding interest in next-generation nuclear reactors. Yet despite this rising awareness, there is a gaping lack in the general knowledge of the fundamental physics and materials science of many of these materials, even for the elemental metals. For accurate modeling of the behavior of these materials, a better understanding of the basic aspects of actinide metals, alloys, and materials is required through experiment and theory. Considerable strides to increase this understanding have indeed been achieved [1-8], but many questions remain. A particularly fundamental question is how the 5*f* electrons fill the $j = 5/2$ and 7/2 levels across the series, i.e., the type of angular momentum coupling that each actinide exhibits [9,10]. To this end, we are systematically investigating the 5*f* states of the elemental actinide metals, since these are the states governing much of the unique electron bonding and physical properties.

The 5*f* states of actinide materials can be directly examined via electron energy-loss spectroscopy (EELS) or x-ray absorption spectroscopy (XAS). With either technique, a core electron is excited above the Fermi energy, directly probing the unoccupied states. Using EELS or XAS excitations from a *d* core level, the 5*f* spin-orbit interaction per hole can be directly examined for a particular actinide material by the spin-orbit sum rule [9-12]. For this analysis, the branching ratio must be extracted from the spin-orbit-split core-level edges in the spectra, which in our case is gathered from the $N_{4,5}$ ($4d \rightarrow 5f$) edges. Electric-dipole selection rules allow two kinds of transitions: N_5 ($4d_{5/2} \rightarrow 5f_{5/2,7/2}$) and N_4 ($4d_{3/2} \rightarrow 5f_{5/2}$). Since an electron from a *d* core state can only be excited into specific 5*f* states, this leads to differences in the branching ratio that can be interrogated using the spin-orbit sum rule.

In this brief communication, we employ EELS in a transmission electron microscope (TEM), combined with many-electron atomic calculations and the spin-orbit sum rule to examine

the electronic structure of the 5*f* states in the ground-state phase of Th, U, Np, Pu, Am, and Cm metal by means of the $N_{4,5}$ transition. The spectra of Th, U, and Pu were shown previously [9,10], but here new spectra for Np, Am, and Cm are given. The branching ratio of the $N_{4,5}$ EELS spectra, and in turn the spin-orbit sum rule analysis, reveal that while the light actinide U exhibits *LS* coupling, the middle actinides Pu, Am, and Cm exhibit intermediate coupling. Data for Cm shows a large shift in the angular-momentum coupling mechanism toward the *LS* limit, a fact that solidifies the spin-orbit sum rule is indeed accurate in describing the 5*f* states. Further, the experimental EELS data for Pu, Am, and Cm fit the intermediate coupling model exceedingly well, thus supporting that the valence for each metal is at, or near, 5, 6, and 7, respectively. Finally, the data also show that the branching ratio is sensitive to delocalization. This is illustrated in the transition from *LS* to intermediate coupling between U and Pu, with Np falling in the middle of the two curves. Pertaining to methods of experiment and theory, EELS experiments in the TEM [9,10] and atomic calculations [11,12] were performed in a manner similar to the references cited.

The $N_{4,5}$ edge for each metal is shown in Fig. 1, where each spectrum is normalized to the N_5 ($4d_{5/2}$) peak height. Immediately noticeable is the gradually growing separation between the N_4 and N_5 peaks from Th to Cm, in pace with the increase in 4*d* spin-orbit splitting with atomic number. Also noticeable is that the N_4 ($4d_{3/2}$) peak reduces in intensity going from Th to Am, but then the trend reverses, giving a larger intensity for Cm. The behavior of the N_4 peak in the EELS spectra in Fig. 1 directly reflects the filling of the angular momentum levels in the 5*f* state. Selection rules govern that a $d_{3/2}$ electron can only be excited into an empty $f_{5/2}$ level, which means that the ratio of the N_4 ($d_{3/2}$) and N_5 ($d_{5/2}$) peak intensities serves as a measure for the relative occupation of the $5f_{5/2}$ and $5f_{7/2}$ levels. The N_4 peak reduces rapidly as the atomic number

increases because the majority of the 5*f* electrons are occupying the $f_{5/2}$ level. By the time Am is reached, the N_4 peak is almost extinct since the $f_{5/2}$ level is close to full with six 5*f* electrons (there is only a minor amount of electrons in the $f_{7/2}$ level). Thus, there is little room for an electron from $d_{3/2}$ to be excited into the $5f_{7/2}$ level. For Cm, the N_4 peak then increases relative to the N_5 peak for particular reasons discussed below.

For the *f* shell, the number of electrons, n_f, and the expectation value of the angular part of the spin-orbit interaction, $\langle w^{110} \rangle$, is given as

$$n_f = n_{7/2} + n_{5/2}, \tag{1}$$

$$\left\langle w^{110} \right\rangle \equiv \tfrac{2}{3} \left\langle l \cdot s \right\rangle = n_{7/2} - \tfrac{4}{3} n_{5/2}, \tag{2}$$

where $n_{7/2}$ and $n_{5/2}$ are the electron occupation numbers of the angular-momentum levels j = 7/2 and 5/2 [9-12]. Thus, $\langle w^{110} \rangle$ reveals the proper angular momentum coupling scheme for a given material. The branching ratio $B = I(N_5)/[I(N_5) + I(N_4)]$ is obtained by calculating the second derivative of the raw EELS spectra, then integrating the area beneath the N_5 and N_4 peaks above zero, which yields the integrated intensities $I(N_5)$ and $I(N_4)$ [13]. The experimental branching ratio for Th, U, Np, Pu, Am, and Cm metal are listed in Table I. For each metal the value of the branching ratio is fed into the spin-orbit sum-rule, yielding the spin-orbit interaction per hole [12]. For the $d \rightarrow f$ transition, the sum rule is given as

$$\frac{\left\langle w^{110} \right\rangle}{14 - n_f} - \Delta = -\frac{5}{2}\left(B - \frac{3}{5} \right), \tag{3}$$

where Δ represents a small correction term for the sum rule calculated using Cowan's relativistic Hartree-Fock code [9,14]. Table I lists the spin-orbit interaction per hole and the correction factor for each actinide metal.

In order to visualize the spin-orbit analysis of the EELS spectra in relation to our atomic

calculations, both are shown on a plot of $<w^{110}>/(14-n_f) - \Delta$ as a function of the number of *f* electrons in Fig. 2(a). The curves for the three theoretical angular-momentum coupling schemes, *LS*, *jj*, and intermediate, as calculated using a many-electron atomic model, are plotted as a short-dashed, long-dashed, and solid line, respectively. The EELS results are indicated by the blue points. Th metal falls on all three curves, which is due to the fact that it takes two electrons to tangle and with less than one 5*f* electron in Th there is no difference between the coupling mechanisms. U falls directly on the *LS* coupling curve, Np between the *LS* and intermediate curve, and Pu, Am, and Cm all fall on or near the intermediate coupling curve. The intermediate curve is strongly shifted towards the *jj* limit for Pu and Am, evidencing the strong preference of the 5*f* electrons for the $5f_{5/2}$ level in these two metals [9,10,15,16]. However, at Cm there is a sudden and pronounced shift in the intermediate coupling curve toward the *LS* limit.

We can calculate the electron occupation numbers $n_{7/2}$ and $n_{5/2}$ by substituting the values of n_f and $<w^{110}>$ in Eqs. (1) and (2). The experimental and theoretical results are listed in Table I and displayed in Fig 2(b), where the number of electrons in the $5f_{5/2}$ and $5f_{7/2}$ levels as calculated in intermediate coupling using the atomic model are drawn with black and red lines, respectively. Again, the experimental EELS results are indicated with blue points. Apart from the slight deviation in the lighter actinides, U and Np, which is caused by delocalization of the 5*f* states and thus indicates a departure from the atomic model, the EELS results are in excellent agreement with the theoretical curves. Figure 2(b) clearly shows that for the actinide metals up to and including Am, the 5*f* electrons strongly prefer the $5f_{5/2}$ level. However, this changes in a striking manner at Cm, where not only does the electron occupation sharply increases for the $5f_{7/2}$ level, but even *decreases* for the $5f_{5/2}$ level. The results shown in Figs. 1 and 2 lead to several conclusions, each of which will be addressed in turn.

The spin-orbit sum rule is sensitive to the degree of delocalization. This was previously alluded to Ref. 9, but here it is solidified by the Np results. The early actinide metals, particularly U, exhibit *LS* coupling. However, the middle actinide metals Pu, Am, and Cm adhere to intermediate coupling. Most interesting is the transition that occurs between U and Pu, where the EELS results change from a pure *LS* coupling for U to a pure intermediate coupling for Pu with Np falling in between these curves (slightly biased towards intermediate coupling). This shows that the branching ratio is sensitive to the degree of delocalization of the 5*f* states. An *LS* mechanism is clearly observed in the more delocalized U metal, but as the 5*f* states become progressively more localized the coupling mechanism shifts towards intermediate coupling, being directly on the intermediate coupling curve by Pu.

These results illustrate that Pu metal is not quite as delocalized as previously believed. In solids with localized states, a pure intermediate coupling mechanism would be expected, and this is exactly what α-Pu metal exhibits in Figs. 1 and 2. This is in fact true for both α- and δ-Pu, since previous branching ratio and spin-orbit sum rule analysis revealed only a minor difference between the two phases [15]. Thus, while the spin-orbit sum rule is sensitive to the degree of delocalization between each individual element, the change in localization between α- and δ-Pu is near the limit of detectibility with the present technique.

Intermediate coupling for the 5f states as obtained from atomic calculations is the appropriate scheme for Pu, Am, and Cm. Although the early actinide metals deviate from the intermediate coupling curve due to delocalization, Fig. 2(a) shows that the middle actinide metals fall directly on it. Once the metals adopt intermediate coupling (from Pu to Cm) the curve in Fig. 2(a) is exceedingly accurate and this is clearly proven by the results for curium. Pu and Am exhibit intermediate coupling that is strongly shifted towards the *jj* limit. In *jj* coupling the

electrons first fill the $f_{5/2}$ level, which can hold no more than six, then begin to fill the $f_{7/2}$ level. This means that in *jj* coupling the maximal energy gain due to spin-orbit interaction is obtained for Am f^6, where the $f_{5/2}$ level is close to full (there is some electron occupation in the $f_{7/2}$ level). For Cm f^7 at least one electron must occupy the $f_{7/2}$ level. The f^7 configuration obtains maximal energy stabilization due to exchange interaction, with all spins parallel in the half-filled shell, and this can only be achieved in *LS* coupling. Thus, the intermediate curve is strongly shifted toward the *LS* limit, as seen in Fig. 2(a), to accommodate the first Hund's rule. For Pu, Am, and Cm the spin-orbit and exchange interaction compete with each other, resulting in intermediate coupling, and this is why Am f^6 still exhibits a very small N_4 peak in the EELS spectrum. However, increasing n_f from 6 to 7, a clear and pronounced shift from optimal spin-orbit stabilization for f^6 to optimal exchange interaction stabilization for f^7 is observed. Accordingly, the N_4 peak in the Cm EELS spectrum becomes once again larger, similar to the actinide metals prior to Am. The change in electron occupation number at Cm is in fact so strong that, compared to Am, not one but two electrons are transferred to the $f_{7/2}$ level in Cm, as seen in Table I and Fig. 2(b). This large change in the 5*f* electron occupation numbers of the angular-momentum states directly influences the magnitude of the magnetic moment exhibited by Cm, and this in turn affects the crystal structure of the metal [17].

Pu, Am, and Cm metal are near $5f^5$, $5f^6$, and $5f^7$, respectively. While the number of 5*f* electrons is not an output of our EELS and spin-orbit analysis, the results in Figs. 1 and 2 for Pu, Am, and Cm metal clearly show that the 5*f* count is at or near 5, 6, and 7, respectively. This is directly attributed to how well the EELS data tracks the intermediate coupling curve for these metals, and exhibits the large change in angular-momentum state occupancy between Am and Cm. In the case of Pu, it has recently been shown using dynamical mean field theory [18] that

the 5*f* count is 5.2, which the authors derive using the branching ratio of the calculated $N_{4,5}$ X-ray absorption spectrum. In addition, new [17,19] and previous [9,10,15,16] experimental and theoretical data indicate an *f*-count at or near 5 for Pu. For Am metal, an *f*-count of 6 is observed in theoretical calculations [20] and via experiments by the lack of magnetism in the metal [21]. This, in turn, begs the question if Pu is $5f^5$, why then is there no experimentally observed magnetism in any of the six allotropic phases of the metal [22]? The lack of magnetism for Am is obvious, since it has a nearly filled j=5/2 level (total angular momentum J = 0), but Pu, which has one hole in the j=5/2 level is vexing. Some mechanism – Kondo shielding, pairing correlations, etc. – must be obfuscating the moment that should be produced by the hole in the j=5/2 level of Pu. Indeed, recent magnetic susceptibility measurements have shown that localized magnetic moments on the order of 0.05 μ_B/atom form in Pu as damage accumulates due to self-irradiation [23]. This suggests that small perturbations to the gentle balance of electronic and magnetic structure of Pu metal may destroy or degrade possible screening effects of a moment due to the hole in the j=5/2 level. Finally, Cm is clearly an f^7 configuration, as supported by experiment [6,17] and theory [18].

This work was performed under the auspices of U.S. Department of Energy by the University of California, Lawrence Livermore National Laboratory under contract No. W-7405-Eng-48 and by DE-AC05-00OR22725 with ORNL, operated by UT-Battelle.

References:

[1] Y. Baer and J. K. Lang, Phys. Rev. B, **21**, 2060 (1980).
[2] G. H. Lander, E. S. Fisher, and S. D. Bader, Adv. Phys. **43**, 1 (1994).
[3] S. Y. Savrasov and G. Kotliar, Phys. Rev. Lett. **84**, 3670 (2000).
[4] L. Havela, T. Gouder, F. Wastin, and J. Rebizant, Phys. Rev. B **65**, 235118 (2002).
[5] J. Wong, M. Krisch, D. L. Farber, F. Occelli, A. J. Schwartz, T.-C. Chiang, M. Wall, C. Boro, and R. Xu, Science **301**, 1080 (2003).
[6] S. Heathman R. G. Haire, T. Le Bihan, A. Lindbaum, M. Idiri, P. Normile, S. Li, R. Ahuja, B. Johansson, and G. H. Lander, Science **309**, 110 (2005).
[7] K. T. Moore, P. Söderlind, A. J. Schwartz, and D. E. Laughlin, Phys. Rev. Lett **96**, 206402 (2006).
[8] M. E. Manley, M. Yethiraj, H. Sinn, H. M. Volz, A. Alatas, J. C. Lashley, W. L. Hults, G. H. Lander, and J. L. Smith, Phys. Rev. Lett. **96**, 125501 (2006).
[9] G. van der Laan, K. T. Moore, J. G. Tobin, B. W. Chung, M. A. Wall, and A. J. Schwartz, Phys. Rev. Lett. **93**, 097401 (2004).
[10] K. T. Moore, G. van der Laan, J. G. Tobin, B. W. Chung, M. A. Wall, and A. J. Schwartz, Ultramicroscopy **106**, 097401 (2006).
[11] G. van der Laan and B. T. Thole, Phys. Rev. B **53**, 14458 (1996).
[12] B. T. Thole and G. van der Laan, Phys. Rev. A **38**, 1943 (1988); Phys. Rev. B **38**, 3158 (1988).
[13] Electron diffraction and imaging of the Am sample in the TEM showed that it contained heavy amounts of stacking faults, which can be argued produces a combination of α and β phases as it is simply a change in the 111 plane stacking. However, spectra taken from areas with varying amounts of stacking faults showed no detectable difference in branching ratio. Thus, α- and β-Am should have very similar $N_{4,5}$ spectra and, in turn, branching ratios.
[14] R. D. Cowan, *The Theory of Atomic Structure and Spectra* (University of California Press, Berkeley, 1981).
[15] K. T. Moore, G. van der Laan, R. G Haire, M. A. Wall, and A. J. Schwartz, Phys. Rev. B **73**, 033109 (2006).
[16] K. T. Moore, M. A.Wall, A. J. Schwartz, B. W. Chung, D. K. Shuh, R. K. Schulze, and J. G. Tobin, Phys. Rev. Lett. **90**, 196404 (2003).
[17] K. T. Moore, G. van der Laan, R. G Haire, M. A. Wall, and A. J. Schwartz, P. Söderlind, Phys. Rev. Lett., in review.
[18] J. H. Shim, K. Haule, and G. Kotliar, Nature **446**, 513 (2007).
[19] J. G. Tobin, P. Söderlind, A. Landa, K. T. Moore, A. J. Schwartz, B. W. Chung, M. A. Wall, J. M. Wills, R. G. Haire, and A. L. Kutepov, Phys. Rev. B, in review.
[20] P. Söderlind and A. Landa, Phys. Rev. B **72**, 024109 (2005).
[21] P. Graf, B. B. Cunningham, C. H. Dauben, J. C. Wallmann, D. H. Templeton, and H. Ruben, J. Am. Chem Soc. **78**, 2350 (1956).
[22] J. C. Lashley, A. Lawson, R. J. McQueeney, and G. H. Lander, Phys. Rev. B **72**, 054416 (2005).
[23] S. K. McCall, M. J. Fluss, B. W. Chung, M. W. McElfresh, D. D. Jackson, and G. F. Chapline, Proc. Natl. Acad. Sci. USA **103**, 17179 (2006).

Table I: The expected number of 5*f* electrons, n_f, the experimental branching ratio, B, of the $N_{4,5}$ EELS spectra, and the expectation value of the 5*f* spin-orbit interaction per hole, $\langle w^{110} \rangle/(14-n_f) - \Delta$, obtained using Eq. (3) for the α phase of Th, U, Np, Pu, Am, and Cm metal. Each branching ratio value is an average of between 10 to 20 EELS spectra, with the standard deviation given in parenthesis. The sum rule requires a small correction factor, which is Δ = -0.017, -0.010, -0.050, 0.000, 0.005, and 0.015 for n_f = 1, 3, 4, 5, 6, and 7, respectively. The experimental electron occupation numbers $n_{5/2}$ and $n_{7/2}$ of the $f_{5/2}$ and $f_{7/2}$ levels are obtained by solving Eqs. (1) and (2).

Metal	n_f	Branching ratio (B)	$\langle w^{110} \rangle/(14-n_f)-\Delta$	$n_{5/2}$	$n_{7/2}$
Th	0.6	0.646 (003)	-0.115 (008)	0.59	0.01
U	3	0.686 (002)	-0.215 (005)	2.28	0.71
Np	4	0.740 (005)	-0.350 (013)	3.22	0.78
Pu	5	0.826 (010)	-0.565 (025)	4.32	0.67
Am	6	0.930 (005)	-0.830 (013)	5.38	0.62
Cm	7	0.794 (003)	-0.485 (008)	4.41	2.59

Figure Captions

Fig. 1: The $N_{4,5}$ EELS spectra for Th, U, Np, Pu, Am, and Cm metal, each normalized to the N_5 peak height. Note the N_4 ($4d_{5/2}$) edge gradually decreases in intensity relative to the N_5 ($4d_{3/2}$) edge going from Th to Am, then increases again for Cm.

Fig. 2 (color online): (a) Plot of the ground-state spin-orbit interaction per hole, $\langle w^{110} \rangle/(14-n_f)-\Delta$, as a function of the number of 5*f* electrons (n_f). The three theoretical angular momentum coupling schemes are shown: *LS*, *jj*, and intermediate. The blue points indicate the results of the spin-orbit analysis using the experimentally measured branching ratios of each metal in Fig. 1. (b) Electron occupation numbers $n_{5/2}$ (solid black line) and $n_{7/2}$ (solid red line) calculated in intermediate coupling as a function of n_f. The blue points again indicate the experimental results: the ground-state $n_{5/2}$ and $n_{7/2}$ occupation numbers of the 5*f* shell from the spin-orbit analysis of the EELS spectra in Fig. 1.

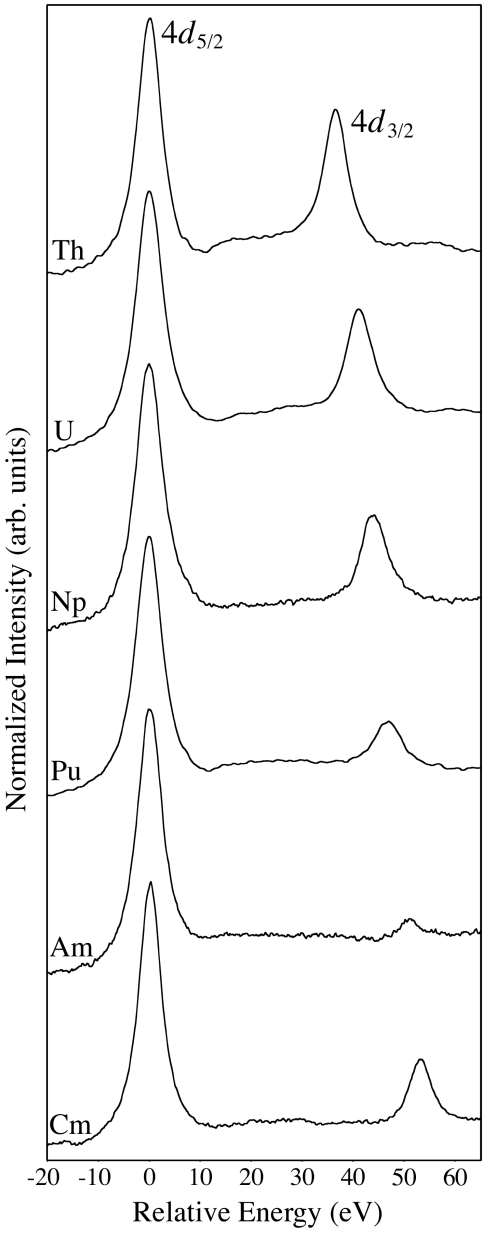

Figure 1 BEJ1062 08MAY2007

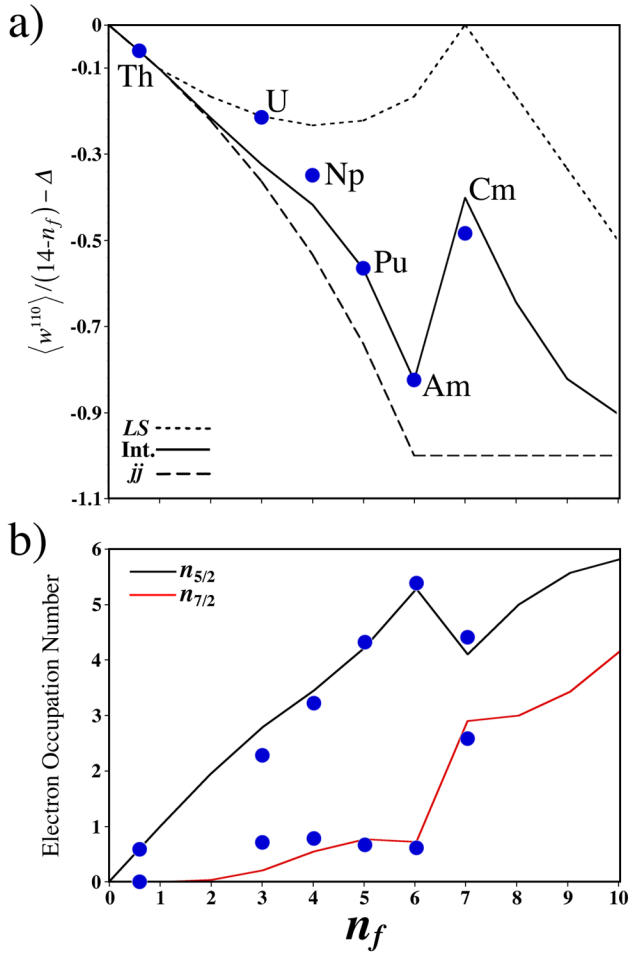

Figure 2 BEJ1062 08MAY2007